Biochimica et Biophysica Acta 1840 (2014) 3115–3122

Contents lists available at ScienceDirect

Biochimica et Biophysica Acta

journal homepage: www.elsevier.com/locate/bbagen

A Fourier transform infrared spectroscopy study of cell membrane domain modifications induced by docosahexaenoic acid

Paolo Mereghetti [a,1], Paola Antonia Corsetto [b,1], Andrea Cremona [b], Angela Maria Rizzo [b], Silvia Maria Doglia [c,d,e], Diletta Ami [c,d,e,*]

[a] Center for Nanotechnology Innovation @NEST, Italian Institute of Technology, Piazza San Silvestro 12, Pisa 56127, Italy
[b] Department of Pharmacological and Biomolecular Sciences, BBFI, Università degli Studi di Milano, via D. Trentacoste 2, 20134 Milano, Italy
[c] Department of Physics, University of Milano-Bicocca, Piazza della Scienza 3, Milano 20126, Italy
[d] Department of Biotechnology and Biosciences, University of Milano-Bicocca, Piazza della Scienza 2, Milano 20126, Italy
[e] Consorzio Nazionale Interuniversitario per le Scienze fisiche della Materia (CNISM) UdR Milano-Bicocca, Milano 20126, Italy

ARTICLE INFO

Article history:
Received 9 April 2014
Received in revised form 25 June 2014
Accepted 2 July 2014
Available online 10 July 2014

Keywords:
ATR-FTIR spectroscopy
Cholesterol
Detergent resistant membranes
DHA
Multidimensional scaling
Sphingomyelin

ABSTRACT

Background: Detergent resistant membranes (DRMs) are a useful model system for the *in vitro* characterization of cell membrane domains. Indeed, DRMs provide a simple model to study the mechanisms underlying several key cell processes based on the interplay between specific cell membrane domains on one hand, and specific proteins and/or lipids on the other. Considering therefore their biological relevance, the development of methods capable to provide information on the composition and structure of membrane domains and to detect their modifications is highly desirable. In particular, Fourier transform infrared (FTIR) spectroscopy is a vibrational tool widely used for the study not only of isolated and purified biomolecules but also of complex biological systems, including intact cells and tissues. One of the main advantages of this non-invasive approach is that it allows obtaining a molecular fingerprint of the sample under investigation in a rapid and label-free way.
Methods: Here we present an FTIR characterization of DRM fractions purified from the human breast cancer cells MCF-7, before and after treatment with the omega 3 fatty acid docosahexaenoic acid (DHA), which was found to promote membrane microdomain reorganization.
Results and Conclusions: We will show that FTIR spectroscopy coupled with multivariate analysis enables to monitor changes in the composition of DRMs, induced in particular by the incorporation of DHA in cell membrane phospholipids.
General significance: This study paves the way for a new label-free characterization of specific membrane domains within intact cells, which could provide complementary information to the fluorescence approaches presently used.

1. Introduction

Membrane microdomains are often isolated from cells as detergent resistant membranes (DRMs), which provide a simple system for the *in vitro* characterization of membrane domain modifications [1–4]. Detergence resistance (DR) refers to the biochemical purification method based on the use of non-ionic detergents, such as Triton X-100, that leads to the isolation of low buoyant density domains. Indeed, DR implies that some membrane fractions are not completely solubilized, but remain in bilayer fragments due to their physico-chemical properties. It should be noted that the composition of DRMs is highly heterogeneous since it strongly depends on the extraction protocol, as well as on the cell type. However, they share a few common properties, such as their enrichment in sphingolipids and cholesterol, and the presence of flotillin-1 among the different proteins, mostly from the plasma membrane, that are associated with these domains [1,4].

In recent years, DRMs gained the attention in different fields of biology since they could represent a simple system to explore the so-called "raftophilicity" of proteins [1], as well as a model system of general value to understand protein–lipid interactions [2]. In this perspective, DRM characterization can provide clues about the mechanisms underlying several crucial cell processes, such as signal transduction and protein sorting [1–4].

Abbreviations: ATR-FTIR, attenuated total reflection-Fourier transform infrared; HP-TLC, high performance-thin layer chromatography; MDS, multidimensional scaling; DR, detergent resistance; DRMs, detergent resistant membranes; AA, arachidonic acid; DHA, docosahexaenoic acid; EPA, eicosapentaenoic acid; CER, ceramide; CHOL, cholesterol; GM1, monosialo ganglioside GM1 ($II^3Neu5AcGg_4Cer$); SM, sphingomyelin; PC, phosphatidylcholine; PE, phosphatidylethanolamine; PI, phosphatidylinositol; PS, phosphatidylserine; PUFA, polyunsaturated fatty acid

* Corresponding author at: Department of Physics, University of Milano-Bicocca, Piazza della Scienza 2, Milano 20126, Italy. Tel.: +39 02 64483461.
E-mail address: diletta.ami@unimib.it (D. Ami).

[1] These authors contributed equally to this work.

http://dx.doi.org/10.1016/j.bbagen.2014.07.003
0304-4165/

Many efforts have been made to develop methods able to characterize *in situ* membrane domains, to get new insights on their structure, function and dynamics in living cells. Among them, for instance, recent developments of super-resolution fluorescence microscopies made it possible to obtain molecular and spatio-temporal information on lipid–lipid and lipid–protein interactions within microdomains [5,6]. A complementary approach to fluorescence microscopies is Fourier transform infrared (FTIR) spectroscopy, which is able to provide a chemical fingerprint of the sample under investigation in a label-free and rapid way. In particular, this vibrational tool allows obtaining information on the composition and structure not only of the main isolated biomolecules [7–12], but also of complex biological systems, including intact cells and tissues [13–19].

A necessary prerequisite to perform IR studies *in situ* is, however, the unambiguous identification of marker bands due to membrane domain components. To this aim, here we applied attenuated total reflection (ATR) FTIR spectroscopy [11,20–22] supported by multivariate statistical analysis [23–25] to study DRMs purified from the MCF7 human breast cancer cells, before and after treatment with the omega 3 fatty acid docosahexaenoic acid (DHA). We chose this system as model for our FTIR study since it has been found that the incorporation of this long chain polyunsaturated fatty acid (PUFA) in MCF7 cell membrane microdomains modifies their physico-chemical properties, strongly impacting on cell functions [26]. Noteworthy, it has been reported that long-chain n − 3 PUFAs, including DHA, inhibit cancer growth as observed in several human cancer cell lines [27,28]. In particular, it has been found that the incorporation of DHA in MCF7 breast cancer cells leads to a significant modification of several membrane microdomain properties, such as the unsaturation degree of the phospholipids, as well as the sphingomyelin and cholesterol content, with important consequences on cell behavior [26].

In the present study, to better assign the IR response of DRMs to well-defined lipid molecules we also measured selected lipid standards, whose content is known to vary after the cell treatment with DHA [26].

Interestingly, this ATR-FTIR study provided information on the variation of some specific components of DRMs, induced by the treatment with the omega 3 fatty acid, in agreement with the biochemical analysis performed on the same system [26].

We believe that the possibility to monitor the modifications in DRMs by FTIR spectroscopy could pave the way for studying changes of the physico-chemical properties of membrane microdomains within intact cells, thus providing a new tool to investigate in a non-invasive way their role in different biological processes.

2. Materials and methods

2.1. Materials

DHA (cis-4,7,10,13,16,19-docosahexaenoic acid sodium salt) and lipid standards were purchased from Sigma-Aldrich (USA). DHA was dissolved in ethanol and stored at − 80 °C under N_2 (g). The rabbit polyclonal anti-flotillin-1 and the mouse monoclonal anti-clathrin heavy chain (HC) antibodies were purchased from Santa Cruz Biotechnology Inc. (Santa Cruz, CA, USA). Bound primary antibody is visualized by proper secondary horseradish peroxidase (HRP)-linked antibody, purchased from Santa Cruz Biotechnology Inc.

2.2. Cell culture conditions

Human breast cancer cells MCF-7 (estrogen receptor-positive) were routinely maintained in DMEM medium (Gibco-BRL, Life Technologies Italia Srl, Italy) supplemented with 10% fetal bovine serum (FBS), 100 U/ml penicillin, 100 mg/ml streptomycin, and 2 mM glutamine.

During treatments the culture medium contained 10% FBS (medium for treatments). Cells were grown at 37 °C in 5% CO_2 at 98% relative humidity.

Cells were treated with DHA for 72 h as previously described [29]. Experiments included control cells which were not exposed to any exogenous fatty acids, but to an equal concentration of ethanol.

2.3. DRM isolation

After treatment, cells were harvested by scraping in phosphate-buffered saline solution containing 0.4 mM Na_3VO_4. Cells were then centrifuged and suspended in 1.4 ml lysis buffer (1% Triton X-100, 10 mM Tris buffer, pH 7.5, 150 mM NaCl, 5 mM EDTA (ethylenediaminetetraacetic acid), 1 mM Na_3VO_4, 1 mM phenylmethylsulfonyl fluoride, 75 mU/ml aprotinin), allowed to stand on ice for 20 min, and finally treated with Dounce homogenizer (10 strokes, tight).

To isolate DRMs, cell lysate was centrifuged (5 min at 1300 *g*) and the supernatant transferred to Eppendorf tubes. 1 ml of lysate was mixed in ultracentrifuge tubes (Beckman Coulter) with equal volume of 85% sucrose (*w*/*v*) in 10 mM Tris buffer, pH 7.5, 150 mM NaCl, 5 mM EDTA, and 1 mM Na_3VO_4, and then overlaid with 5.5 ml of 30% *w*/*v* sucrose (in the previous buffer) and 4 ml of 5% *w*/*v* sucrose. Tubes were centrifuged at 200,000 *g*, for 17 h at 4 °C (Optimal LE-80K Ultracentrifuge, Beckman Coulter). After centrifugation, 11 fractions were collected; to confirm the location of DRMs, the content of cholesterol (CHOL), sphingomyelin (SM), and gangliosides was determined in each fraction by high performance thin layer chromatography (HP-TLC) and of flotillin-1 and clathrin by western blot, as previously described in [26].

To prepare the samples for ATR-FTIR analysis the DRM fraction was dialyzed for 8 h at 4 °C in distilled water upon stirring, using dialysis tubes with MW cutoff 12.000–14.000 (Spectra/Pore Spectrum Medical Industries, USA), and changing the water every 30 min.

2.4. ATR-FTIR spectroscopy analysis

FTIR absorption spectra of DRMs, before and after the cell treatment with DHA, were collected in ATR mode, using a single reflection diamond element (Golden Gate, Specac, USA).

In particular, the sample is placed in contact with a high refractive diamond element. The IR beam reaches the interface between the ATR support and the sample at an angle larger than that corresponding to the beam total reflection. In this way, the beam is totally reflected by the interface and penetrates into the sample as an evanescent wave, where it can be absorbed. The beam penetration depth is of the order of the IR wavelength (a few microns) and depends on the wavelength, the incident angle, as well as on the refractive indices of the sample and of the ATR element [22].

For our experiments, approximately 5 μl of sample was deposited on the ATR plate and dried at room temperature in order to obtain a homogeneous film. Since some buffer components were found to interfere with the IR response, after evaporation of the solvent we rinsed quickly the DRM film with distilled water, a procedure widely used in the ATR measurements of biomolecules [20,30].

The ATR-FTIR measurements were performed using the Varian 670-IR spectrometer (Varian Australia Pty Ltd., Mulgrave, VIC, Australia) equipped with a nitrogen-cooled Mercury Cadmium Telluride (MCT) detector, under the following conditions: 2 cm^{-1} spectral resolution, a scan speed of 25 kHz, 512 scan coadditions, and triangular apodization. The measured spectra were smoothed by a binomial function (13 points) and second derivative spectra were obtained by the Savitzky Golay method (3rd grade polynomial, 9 smoothing points) [31].

The same parameters have been used for the analysis of lipid standards.

To verify the reproducibility and reliability of the spectral results, three independent DRM preparations were analyzed.

2.5. Multidimensional scaling (MDS)

Given a set of multidimensional objects, the FTIR spectra in our case, a value $\delta_{i,j}$ of dissimilarity between each pairs of data in the set is computed. Usually the Euclidean distance is used as dissimilarity measure. Multidimensional scaling (MDS), also called principal coordinate analysis, projects the original multidimensional objects into a low dimensional space such that the distances among the points in the new space, $d_{i,j}$, match as much as possible the original dissimilarities of $\delta_{i,j}$. For a detailed description of the MDS method, see reference [32]. Multivariate statistical analysis on the measured spectra was performed using the software R [33]. At first, z-score normalization was applied, *i.e.* data were centered by their mean and divided by their standard deviation. The Euclidean distance was used to compute the dissimilarity matrix and the classical multidimensional scaling algorithm was then applied using three dimensions. The assignment of the most relevant wavenumbers has been supported by looking at the value of the pseudo-weights (s) obtained as $s = \sum_{i=1}^{K} \sqrt{\lambda_i} |X^+ p_i|$ where X^+ is the Moore–Penrose pseudo-inverse of the original data (the standardized spectra), p_i is the projection on the i-th dimension, λ_i is the corresponding eigenvalue and K is the number of dimensions considered [34]. The pseudo-weights have been then scaled within the range [0–1]. Due to the pseudo-inversion, the pseudo-weights do not smoothly vary along the wavenumbers but they tend to be sharp peaked lines. To better correlate the pseudo-weights with the IR spectra, we smoothed the pseudo-weights using a Gaussian Kernel smoothing [35].

To assess the change in the distance between DRMs—before and after the DHA treatment—and the lipid standards, the unpaired t-test was applied. The Euclidean distance has been computed using all the available replicas obtaining a set of distances $d(K, S) = \{d(K, S)_j\}$ where K can be the control (CTR) or the treated sample (DHA), S are the lipid standards and j is the replica index. Then, a two sample t-test is performed between d(CTR, S) and d(DHA, S) to check whether the two distances differ at a significance level of 0.05.

3. Results and discussion

3.1. Biochemical characterization of DRMs

DRMs were isolated from control and DHA-treated MCF-7 cells by a sucrose gradient [26]. To characterize and assign DRMs to the proper sucrose fraction, we analyzed by TLC the content of cholesterol (CHOL), and of several sphingolipids, including sphingomyelin (SM) and gangliosides, while we characterized by western blot the presence of flotillin-1 (Flot1) and/or clathrin.

In particular, as shown in Fig. 1 for the control sample, DRMs were isolated in fractions 5 and 6 that contain not only cholesterol, sphingomyelin and specific gangliosides such as GM1, but also the protein marker Flot1, absent in the other fractions [36]. On the contrary, the membrane protein clathrin, a protein highly represented in non-DRM fractions, is recovered in the soluble fraction 11. For the FTIR analysis we utilized the fraction 5, particularly enriched with cholesterol, sphingomyelin and the ganglioside GM1.

3.2. FTIR analysis of DRMs

To explore the potential of FTIR spectroscopy for the characterization of DRM composition, we studied their IR response after extraction from human breast cancer MCF-7 cells, before and after the treatment with DHA.

As shown in Fig. 2, the ATR-FTIR absorption spectrum of DRMs is complex since it is due to the absorption of several biomolecules, including lipids, proteins, and carbohydrates.

In particular, as indicated in the figure, the stretching vibrations of the lipid hydrocarbon tails dominate the spectral range of 3050–2800 cm^{-1}. Between approximately 1500 and 1350 cm^{-1} the deformation modes of the lipid hydrocarbon tails as well as the absorption of several lipid head moieties are instead observed. Moreover, the ester carbonyl absorption is detected around 1740 cm^{-1} [10,12]. In addition, between 1700 and 1500 cm^{-1} the spectrum is dominated by the amide I and amide II bands, mainly due to the C═O stretching and the NH bending of the peptide bond, respectively. Notably, the amide I band is sensitive to the protein secondary structure [7,11]. We should also mention that a complex absorption mainly due to phosphates and carbohydrates occurs in the spectral range of 1250–1000 cm^{-1}, where also the absorption of phospho- and glycosphingo-lipids, as well as that of glycosylated proteins, is observed [9,10,12,37,38]. Finally, the vibrations of several lipid moieties fall between 1000 and 750 cm^{-1}, including the carbon–nitrogen, the single bond P – O stretching modes, the CH_2 rocking, and the CH deformation vibrations [10,12,39].

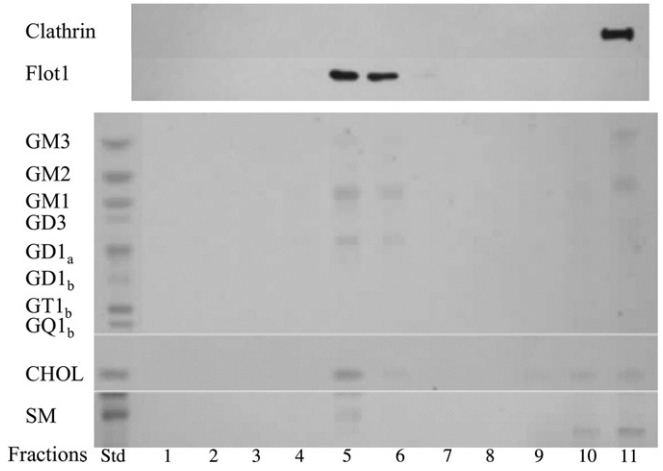

Fig. 1. Biochemical analysis of sucrose gradient fractions from untreated MCF-7 human breast cancer cells. Protein markers clathrin and flotillin-1 (Flot1) were analyzed by western blot. Mono- (GM1, GM2, GM3), di- ($GD1_a$, $GD1_b$, GD3), tri- ($GT1_b$), and tetra- ($GQ1_b$) ganglioside, cholesterol (CHOL) and sphingomyelin (SM) contents were analyzed by HP-TLC.

Interestingly, we found that some spectral features of purified DRMs changed after the DHA treatment. In particular, the detection of these changes was possible by the analysis of second derivative spectra, which allow resolving the overlapping components of the IR absorption bands [31].

3.2.1. Analysis of DRM protein content

Information on the sample protein content was obtained by the IR response of DRMs in the spectral range between 1700 and 1600 cm^{-1} (Fig. 3), which is dominated by the absorption of the amide I band [7,11]. In particular, the second derivative spectrum of DRMs purified from cells before the DHA treatment, taken as a control, is characterized by a strong band at ~1655 cm^{-1}, mainly due to α-helix and random coil structures, and by minor absorptions at ~1694 cm^{-1} due to intramolecular β-sheets, 1684 cm^{-1} assigned to β-turns and ~1635 cm^{-1}, again assigned to intramolecular β-sheets [7,11]. Minor but reproducible variations of the total protein secondary structures of DRMs were observed after the DHA treatment, as indicated in particular by the change in the intensity of the α-helix absorption band. Even if the interpretation of this result at present is not possible, we should underline that this spectral response is a useful tool to verify that no depletion of DRM protein content, induced for instance by the dialysis procedure, occurred during the sample preparation for FTIR analysis. Interestingly, we should note that the amide I spectral features of DRM fraction 5 are different compared to other fractions. For instance, we have reported in Supplemental Fig. 1 the amide I band analysis of fraction 11, which does not represent DRMs (see also Fig. 1).

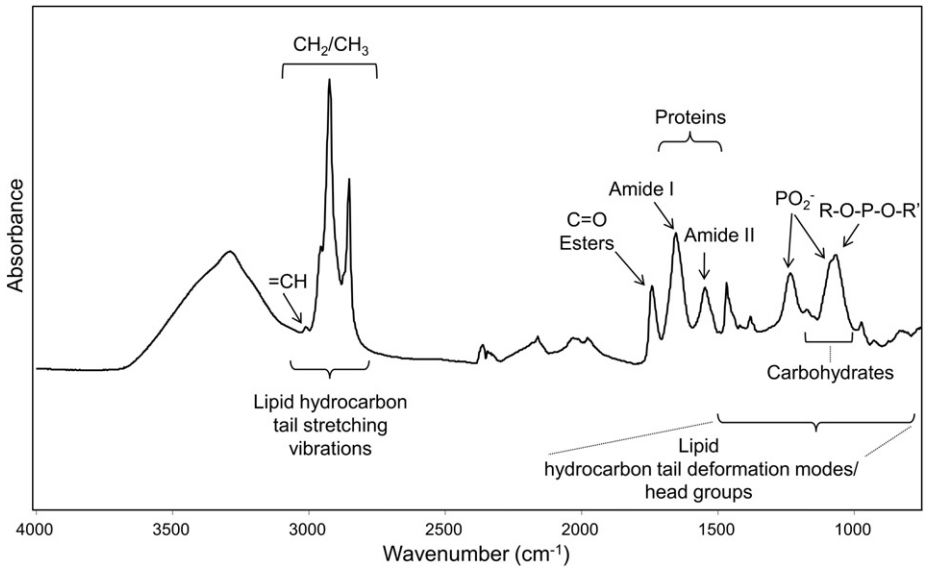

Fig. 2. ATR-FTIR spectrum of DRMs purified from MCF7 control cells. The ATR-FTIR spectrum of DRMs purified from MCF7 cells is reported without any correction. The assignment of the main components is indicated.

3.2.2. Analysis of DRM lipid composition

The lipid absorption in the mid IR is very complex since it is due to the response of the different lipid moieties. For this reason, we will present the lipid analysis of DRMs in different spectral ranges, each due to the absorption of specific vibrational modes.

3.2.2.1. Lipid hydrocarbon tail stretching region. In Fig. 4 the second derivative spectra of DRMs, purified from cells before and after the treatment with DHA, are reported between 3050 and 2800 cm^{-1}.

The spectrum of the control is dominated by four main absorption bands due to the CH_2 (at ~2921, 2851 cm^{-1}) and CH_3 (at ~2957 and 2872 cm^{-1}) stretching vibrations of lipids, in particular due to their hydrocarbon tails [10,12]. Moreover, a low intensity but significant absorption is observed around 3009 cm^{-1}, which is assigned to the ═CH stretching vibration typical of unsaturated fatty acids [12], as can be seen in the enlarged inset of Fig. 4.

Interestingly, the ═CH stretching vibration was found to significantly change after the cell treatment with DHA. In particular, the olefinic group band is more intense and up-shifted of a few wavenumbers, from 3009 to 3013 cm^{-1}, indicating that a higher degree of acyl chain unsaturation is induced by the treatment with DHA [12]. Indeed, the biochemical analysis found that DHA is actually incorporated in DRM phospholipids, leading to an increase of their unsaturation state [26].

3.2.2.2. Analysis of lipid head group modes and hydrocarbon tail deformations. To better explore lipid changes in DRMs possibly induced by the treatment with DHA, we extended the FTIR analysis to the spectral range between 1500 and 1000 cm^{-1} (Fig. 5A and B), where several vibrational modes due to head groups, as well as hydrocarbon tail deformations occur [10,12,38]. In particular, to visualize the most significant spectral changes, we reported the spectra between 1500 and 1350 cm^{-1} (Fig. 5A) and between 1150 and 1000 cm^{-1} (Fig. 5B).

As shown in Fig. 5A, the second derivative spectrum of the DRMs from control cells is characterized by several well-resolved bands, in particular at ~1467 cm^{-1} (CH_2 bending and/or CH_3 deformation), 1436 cm^{-1} (CH_3 deformation), 1417 cm^{-1} (CH_2 deformation),

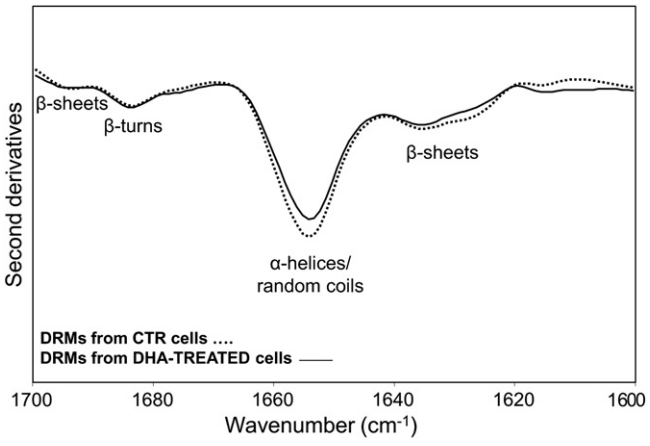

Fig. 3. Amide I band analysis. ATR-FTIR second derivative spectra of DRMs purified from MCF7 cells, before (dotted line) and after (continuous line) treatment with DHA, in the amide I region. Spectra have been normalized at the tyrosine peak intensity (~1515 cm^{-1}) for comparison.

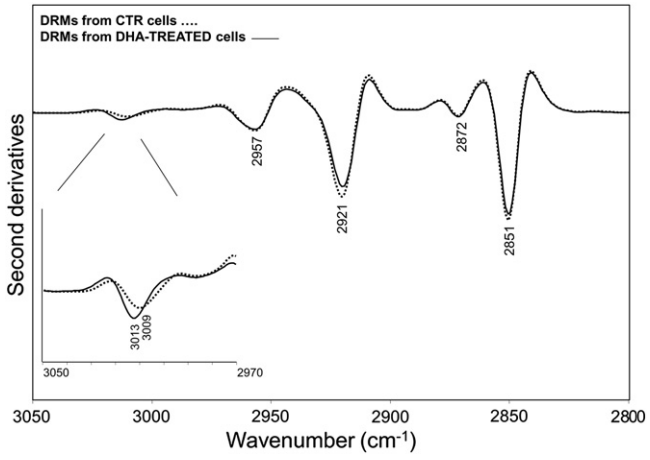

Fig. 4. Analysis of lipid hydrocarbon tail stretching vibrations. ATR-FTIR second derivative spectra of DRMs purified from MCF7 cells, before (dotted line) and after (continuous line) treatment with DHA, in the hydrocarbon tail stretching spectral region. In the inset, a magnification of the olefinic group absorption is reported. Spectra have been normalized at the ~2957 cm^{-1} CH_3 peak intensity for comparison.

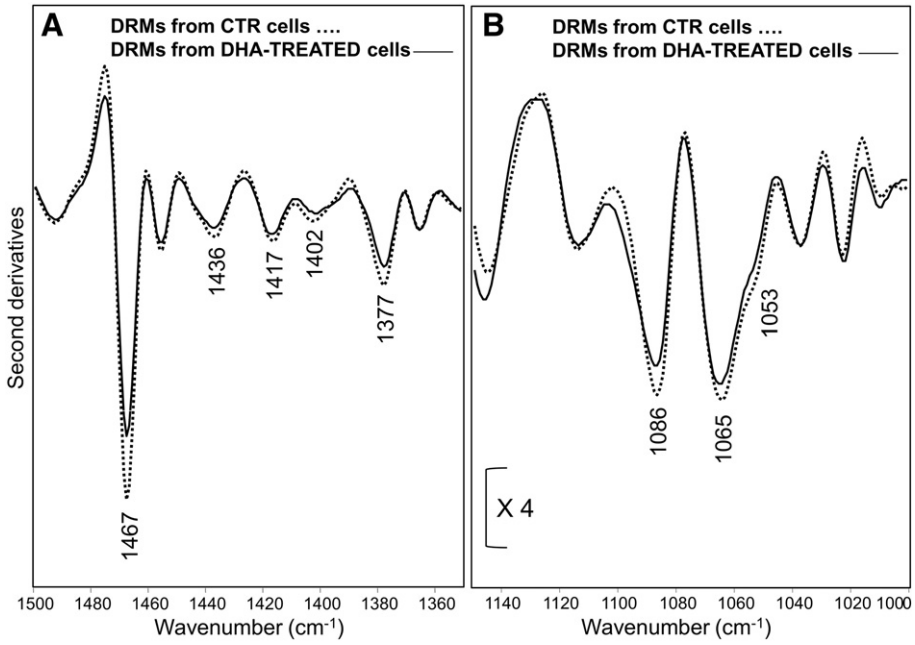

Fig. 5. Analysis of lipid head group modes and hydrocarbon tail deformations. ATR-FTIR second derivative spectra of DRMs purified from MCF7 cells, before (dotted line) and after (continuous line) treatment with DHA. Spectra, displayed between 1500 and 1350 cm^{-1} (A) and between 1150 and 1000 cm^{-1} (B), have been normalized at the tyrosine peak intensity (~1515 cm^{-1}) for comparison. Spectra in panel (B) have been reported in an enlarged intensity scale, as indicated.

1402 cm^{-1} (CH_3 deformation of N $(CH_3)_3$), and ~1377 cm^{-1} (CH_3 deformation) [12,39–41]. Furthermore (see Fig. 5B), we observed a complex band at ~1065 cm^{-1}, which can be assigned to the diester phosphate stretching, with a shoulder around 1053 cm^{-1} due to the C–O stretching of esters [10,12,42]. Moreover, also the absorption of carbohydrates occurs in this spectral range, which can be mainly due to the sugar moiety of some lipids, and/or to glycosylated proteins [9,37,38]. In addition, a well-resolved component occurs at ~1086 cm^{-1}, due to the P═O symmetric stretching of PO_2^- [10,12,42]. Interestingly, the intensities of these bands were found to change in the spectrum of DRMs purified from cells treated with DHA. In particular, following the omega 3 incorporation, the above IR bands were found to decrease in intensity.

3.3. Multidimensional scaling (MDS) of FTIR spectra of DRMs and lipid standards

The FTIR results discussed above indicated that the cell treatment with DHA induced changes in the lipid composition of DRMs, as confirmed by the detailed biochemical analysis recently reported in the literature [26].

Here, we explored the possibility to disclose the most significant lipids responsible for the observed spectral changes. To this aim it has been necessary to support the FTIR analysis with a multivariate analysis approach, namely the multidimensional scaling (MDS) [33], since the IR response of the lipid molecules, whose content might vary in DRMs after DHA treatment, is complex and is characterized by overlapping absorptions.

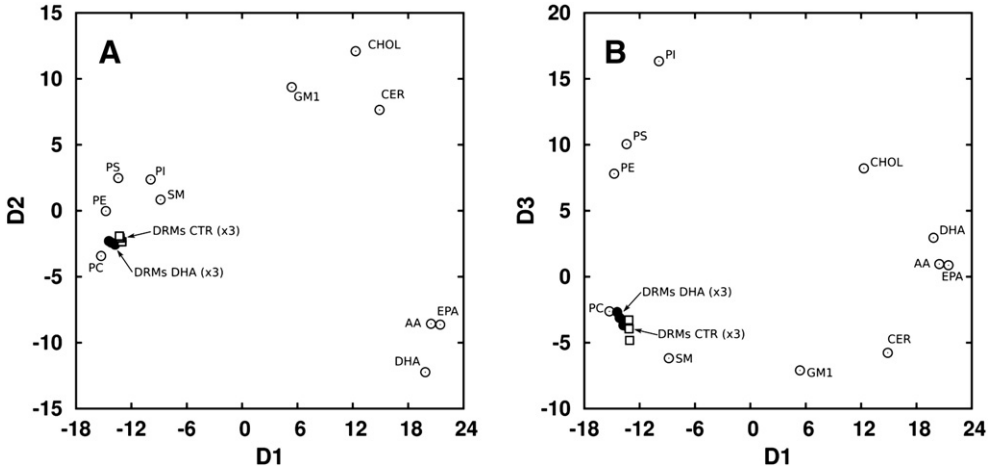

Fig. 6. MDS analysis. MDS 2D plots of DRMs—purified from cells control (empty squares) and treated with DHA (filled circles)—and of the selected lipid standards (empty circles). Repeated DRM symbols indicate the three independent DRM preparations that have been analyzed. Dimensions 1–2 (A) and dimensions 1–3 (B). The analysis has been performed on the measured FTIR spectra between 1500 and 1000 cm^{-1}.

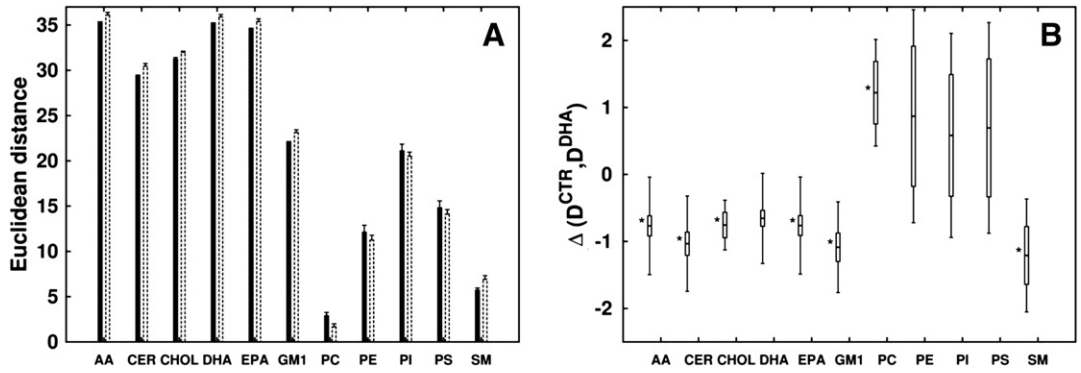

Fig. 7. Euclidean distances and differences in the three dimensional MDS projections. The Euclidean distances in the three dimensional MDS projections (see Fig. 6) have been evaluated for the lipid standards and DRMs before (filled black bars) and after (empty bars) DHA treatment (A). Differences in Euclidean distances between lipid standards and DRMs before and after DHA treatment are shown as empty boxes with error bars (B). A negative value implies that the content of that lipid standard decreases following the cell treatment with DHA. *p*-Values were determined using an unpaired t-test. $^{*}p$-Value < 0.05. Box height indicates the standard deviation around the estimated average value, while the error bar indicates the 95% confidence interval.

In particular, to assign the observed spectroscopic changes to specific lipid molecules, we compared by MDS the DRM measured spectra with the IR response of lipid standards, including several phospholipids, ceramide, the ganglioside GM1, cholesterol, and omega 3 and 6 fatty acids, whose content in DRMs was found to vary after the incorporation of DHA by cells [26].

The choice of MDS was driven by its ability to project the original spectra into a set of low dimensional coordinates, whose Euclidean distances approximate as much as possible the original dissimilarities among the spectra. In this way, the closer are two points in the low dimensional space, the more similar are the corresponding spectra. Analogous results can be obtained using principal component analysis, which is indeed strictly related to MDS [33].

For the sake of clarity, in Supplementary Material we reported the structural formulas of DHA and of the lipid molecules that mainly contributed to the observed spectral variance before and after the DHA treatment (Fig. S2).

3.3.1. MDS in the head group and hydrocarbon tail absorption region

We performed the MDS between 1500 and 1000 cm^{-1} (Fig. 6A and B), a complex spectral range where the IR response of different molecules, including lipids and carbohydrates, overlaps. In particular, different vibrational modes not only due to lipid hydrocarbon tails but also to head groups occur.

The contribution of each lipid standard to the spectral profile of the DRMs is summarized on the MDS projection plots (Fig. 6) where the Euclidean distance between two points is directly proportional to the similarities of the corresponding spectra. As displayed in Fig. 6, the phospholipids, which include the phosphosphingolipid sphingomyelin (SM), contributed to the spectral profiles of both DRMs purified from control and treated cells, more than the other lipid molecules.

To better identify the lipids that contributed mostly to the observed spectral changes, we calculated the Euclidean distances between lipid standards and DRMs from control and DHA-treated cells (Fig. 7A). It has been found that among the analyzed phospholipids

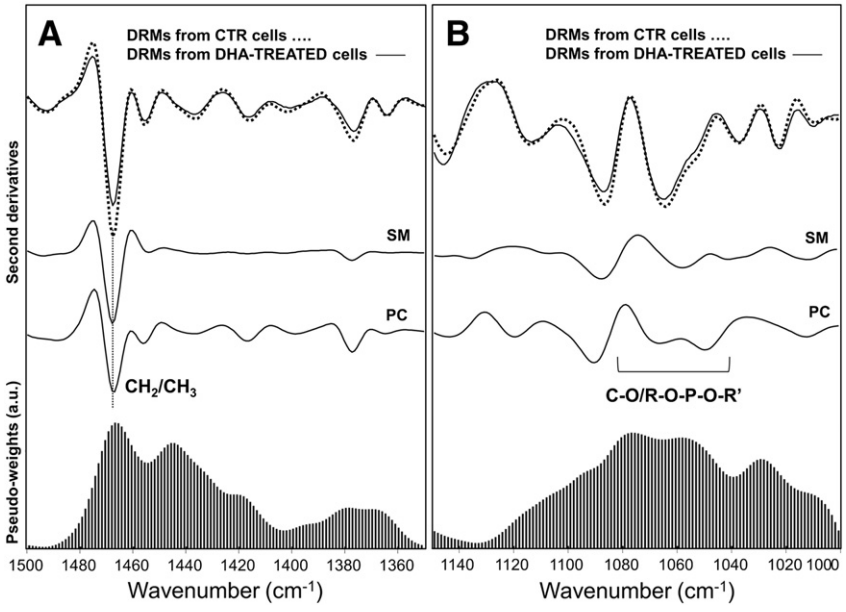

Fig. 8. Contribution of lipid standards to the observed spectral variance of DRMs. The second derivative spectra of DRMs—before and after the DHA treatment—are compared with those of lipid standards mostly contributing to the spectral changes observed after DHA treatment. Spectra, reported between 1500 and 1350 cm^{-1} (A) and between 1150 and 1000 cm^{-1} (B), have been normalized at the ~1515 cm^{-1} tyrosine peak intensity for comparison. Spectra in panel (B) have been reported in an enlarged intensity scale (×4), as in Fig. 5. The standardized MDS pseudo-weights were also reported and the most representative wavenumbers associated with a high weight value are indicated.

phosphatidylcholine (PC) highly contributed to the observed spectral changes between DRMs, control and DHA-treated (Figs. 6 and 7). Furthermore, the role of SM clearly emerged also as one of the most important lipid molecules that determined significant spectral variations after DHA incorporation, and in particular the negative value of its variation indicates that its content decreased following the DHA treatment. We found a ~20% decrease of the SM content compared to the control, which is qualitatively in agreement with the 50% reduction disclosed by the biochemical analysis [26,43]. Interestingly, a decrease in SM content could have important biological implications, as it can affect cell functions [26,43].

In addition, other lipid molecules were found to decrease upon the omega 3 incorporation, such as cholesterol, ceramide and the ganglioside GM1 (Fig. 7A and B).

In Fig. 8 we reported the comparison between the second derivative spectra of DRMs, control and DHA-treated on one hand, and of SM and PC on the other, in the spectral range of 1500–1000 cm^{-1}. In addition, the MDS pseudo-weight plot is also displayed to better visualize the most significant components determining the higher spectral variance observed.

In particular, the components determining the most significant spectral variance are those associated with the CH_3 and CH_2 hydrocarbon tail modes around 1465 cm^{-1} [10,12,38–40], and with the complex absorption approximately between 1080 and 1040 cm^{-1}, mainly due to the overlapping contributions of the phosphate diesters, the CO of the ester group, as well as of carbohydrates [9,10,12,38,42].

3.3.2. MDS analysis of cholesterol in the spectral range between 950 and 750 cm^{-1}

To better investigate the variation of cholesterol content in DRMs following the DHA treatment, we extended the analysis to the spectral range between 950 and 750 cm^{-1}, where several cholesterol marker bands occur, including those due to CH and CH_2 vibrations [12,44].

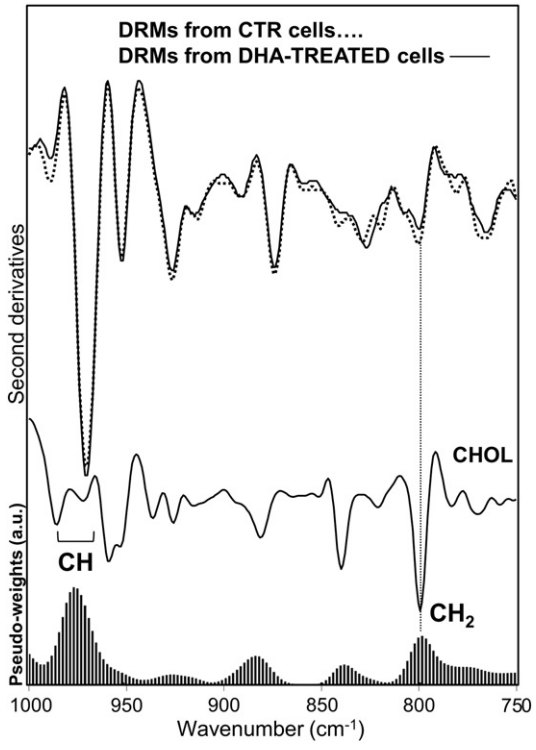

Fig. 9. Contribution of cholesterol to the observed spectral variance of DRMs. The second derivative spectra of DRMs—before and after the DHA treatment—are compared with that of cholesterol, between 950 and 750 cm^{-1}, after normalization at the ~1515 cm^{-1} tyrosine peak intensity. The standardized MDS pseudo-weights were also reported and the most representative wavenumbers associated with a high weight value are indicated.

The difference in the distances between the cholesterol and the DRMs from control and treated cells was found to be negative and significant (p-value < 0.05) (data not shown). This result indicated that cholesterol significantly contributed to the spectral profile of DRMs and that its content decreased following the omega 3 cell treatment, in agreement with the FTIR-MDS analysis performed between 1500 and 1000 cm^{-1}, discussed in Section 3.3.1. In particular, a decrease of ~18% of the cholesterol content compared to the control was found, qualitatively, in agreement with the 40% reduction obtained by the biochemical analysis [26].

Furthermore, to highlight the spectral components responsible of the observed variance, we reported in Fig. 9 the comparison between the second derivative spectra of DRMs—purified from cells before and after the DHA incorporation—and of cholesterol. In addition, the MDS pseudo-weight plot, also displayed in the figure, allowed disclosing that the most significant components distinguishing among the spectra were those at ~975 cm^{-1}, tentatively assigned to C–H deformation modes [12,44], and at ~799 cm^{-1}, assigned to CH_2 bending vibration [44]. As it can be appreciated by the second derivative inspection, the 799 cm^{-1} band was found to decrease following the omega 3 incorporation, reflecting therefore a reduction of the cholesterol content.

Interestingly, this result—confirmed by the FTIR results obtained in the spectral range between 1500 and 1000 cm^{-1}—is in agreement with the biochemical characterization recently reported in literature [26]. Indeed, the authors found that the treatment of MCF7 cells with DHA led to a significant reduction of this sterol in DRMs, with important consequences on their physico-chemical properties and functions [26,45].

4. Conclusions and perspectives

The present study indicates that FTIR spectroscopy supported by multivariate analysis can be a useful technique to monitor changes in the physico-chemical properties of membrane domains such as DRMs, which are considered a valuable model system in cell membrane research [1–4].

In agreement with the detailed biochemical characterization of the same system recently reported in the literature [26], we found that the cell treatment with DHA led to important modifications of membrane domains. Firstly, a significant increase of the unsaturation degree of phospholipid acyl chains was observed. Moreover, the content of sphingomyelin and cholesterol—key components of DRMs—was found to vary after the omega 3 treatment, and in particular DRMs purified from DHA-treated cells displayed a significantly lower amount of sphingomyelin and cholesterol compared to the untreated sample. The decrease of cholesterol content is expected to affect membrane fluidity and cell functions [26,45].

Furthermore, we believe that our FTIR characterization of DRMs could have an additional outcome, namely the possibility to extend the IR study of membrane domains to intact cells, in a non-invasive and label-free way. Indeed, the IR response of intact cells gives information on processes that can take place simultaneously. In this perspective, the FTIR approach could make it possible to correlate variations of membrane domain physico-chemical properties with specific cell events, allowing a better investigation of their biological significance, thus providing complementary information to that given by fluorescence approaches.

Acknowledgements

D.A. acknowledges a postdoctoral fellowship of the University of Milano-Bicocca.

S.M. D. acknowledges the GA (Grandi Attrezzature scientifiche) and FAR (Fondi di Ateneo per la Ricerca) grants of the University of Milano Bicocca for the financial support to the FTIR Spectroscopy Laboratory of the Department of Biotechnology and Biosciences.

A.M. R. is indebted to the Italian Space Agency Grant MARS 500 “Omega-3” for the financial support.

The authors are grateful to Antonino Natalello, of the University of Milano Bicocca, for helpful discussions and suggestions.

Appendix A. Supplementary data

Supplementary data to this article can be found online at http://dx.doi.org/10.1016/j.bbagen.2014.07.003.

References

[1] D.A. Brown, Lipid rafts, detergent-resistant membranes, and raft targeting signals, Physiology 21 (2006) 430–439.
[2] D. Lichtenberg, F.M. Goñi, H. Heerklotz, Detergent-resistant membranes should not be identified with membrane rafts, Trends Biochem. Sci. 30 (2005) 430–436.
[3] L.J. Pike, Lipid rafts: heterogeneity on the high seas, Biochem. J. 378 (2004) 281–292.
[4] K. Simons, W.L.C. Vaz, Model systems, lipid rafts, and cell membranes, Annu. Rev. Biophys. Biomol. Struct. 33 (2004) 269–295.
[5] V. Mueller, A. Honigmann, C. Ringemann, R. Medda, G. Schwarzmann, C. Eggeling, FCS in STED microscopy: studying the nanoscale of lipid membrane dynamics, Methods Enzymol. 519 (2013) 1–38.
[6] D.M. Owen, A. Magenau, D. Williamson, K. Gaus, The lipid raft hypothesis revisited—new insights on raft composition and function from super-resolution fluorescence microscopy, Bioessays 34 (2012) 739–747.
[7] A. Barth, Infrared spectroscopy of proteins, Biochim. Biophys. Acta 1767 (2007) 1073–1101.
[8] M. Banyay, M. Sarkar, A. Gräslund, A library of IR bands of nucleic acids in solution, Biophys. Chem. 104 (2003) 477–488.
[9] M. Kacurakova, R.H. Wilson, Developments in mid-infrared FT-IR spectroscopy of selected carbohydrates, Carbohydr. Polym. 44 (2001) 291–303.
[10] J.L.R. Arrondo, F.M. Goni, Infrared studies of protein-induced perturbation of lipids in lipoproteins and membranes, Chem. Phys. Lipids 96 (1998) 53–68.
[11] L.K. Tamm, S.A. Tatulian, Infrared spectroscopy of proteins and peptides in lipid bilayers, Q. Rev. Biophys. 30 (1997) 365–429.
[12] H.L. Casal, H.H. Mantsch, Polymorphic phase behaviour of phospholipid membranes studied by infrared spectroscopy, Biochim. Biophys. Acta 779 (1984) 381–401.
[13] D. Ami, A. Natalello, S.M. Doglia, Fourier transform infrared microspectroscopy of complex biological systems: from intact cells to whole organisms, Methods Mol. Biol. 895 (2012) 85–100.
[14] S. Caine, P. Heraud, M.J. Tobin, D. McNaughton, C.C. Bernard, The application of Fourier transform infrared microspectroscopy for the study of diseased central nervous system tissue, NeuroImage 59 (2012) 3624–3640.
[15] C. Sandt, O. Féraud, N. Oudrhiri, M.L. Bonnet, M.C. Meunier, Y. Valogne, A. Bertrand, M. Raphaël, F. Griscelli, A.G. Turhan, P. Dumas, A. Bennaceur-Griscelli, Identification of spectral modifications occurring during reprogramming of somatic cells, PLoS One 7 (2012) e30743.
[16] D. Ami, P. Mereghetti, A. Natalello, S.M. Doglia, M. Zanoni, C.A. Redi, M. Monti, FTIR spectral signatures of mouse antral oocytes: molecular markers of oocyte maturation and developmental competence, Biochim. Biophys. Acta 1813 (2011) 1220–1229.
[17] P. Heraud, E.S. Ng, S. Caine, Q.C. Yu, C. Hirst, R. Mayberry, A. Bruce, B.R. Wood, D. McNaughton, E.G. Stanley, A.G. Elefanty, Fourier transform infrared microspectroscopy identifies early lineage commitment in differentiating human embryonic stem cells, Stem Cell Res. 4 (2010) 140–147.
[18] D. Ami, T. Neri, A. Natalello, P. Mereghetti, S.M. Doglia, M. Zanoni, M. Zuccotti, S. Garagna, C.A. Redi, Embryonic stem cell differentiation studied by FT-IR spectroscopy, Biochim. Biophys. Acta 1783 (2008) 98–106.
[19] L.P. Choo, D.L. Wetzel, W.C. Halliday, M. Jackson, S.M. Le Vine, H.H. Mantsch, In situ characterization of beta-amyloid in Alzheimer's diseased tissue by synchrotron Fourier transform infrared microspectroscopy, Biophys. J. 71 (1996) 1672–1679.
[20] A. Natalello, D. Ami, S.M. Doglia, Fourier transform infrared spectroscopy of intrinsically disordered proteins: measurement procedures and data analyses, in: V.N. Uversky, A.K. Dunker (Eds.), Intrinsically Disordered Protein Analysis, Methods in Molecular BiologyHumana Press, 2012, pp. 229–244. http://dx.doi.org/10.1007/978-1-61779-927-3_16.
[21] A. Natalello, A.M. Frana, A. Relini, A. Apicella, G. Invernizzi, C. Casari, A. Gliozzi, S.M. Doglia, P. Tortora, M.E. Regonesi, A major role for side-chain polyglutamine hydrogen bonding in irreversible ataxin-3 aggregation, PLoS ONE 6 (2011) e18789.
[22] E. Goormaghtigh, V. Raussens, J.M. Ruysschaert, Attenuated total reflection infrared spectroscopy of proteins and lipids in biological membranes, Biochim. Biophys. Acta 1422 (1999) 105–185.
[23] D. Ami, P. Mereghetti, S.M. Doglia, Multivariate analysis for Fourier transform infrared spectra of complex biological systems and processes, in: L. Valim de Freitas, A.P. Barbosa Rodrigues de Freitas (Eds.), Multivariate Analysis in Management, Engineering and the SciencesInTech, Rijeka, 2013, pp. 189–220. http://dx.doi.org/10.5772/53850.
[24] J. Trevisan, P.P. Angelov, P.L. Carmichael, A.D. Scott, F.L. Martin, Extracting biological information with computational analysis of Fourier-transform infrared (FTIR) biospectroscopy datasets: current practices to future perspectives, Analyst 137 (2012) 3202–3215.
[25] J.G. Kelly, J. Trevisan, A.D. Scott, P.L. Carmichael, H.M. Pollock, P.L. Martin-Hirsch, F.L. Martin, Biospectroscopy to metabolically profile biomolecular structure: a multistage approach linking computational analysis with biomarkers, J. Proteome Res. 10 (2011) 1437–1448.
[26] P.A. Corsetto, A. Cremona, G. Montorfano, I.E. Jovenitti, F. Orsini, P. Arosio, A.M. Rizzo, Chemical–physical changes in cell membrane microdomains of breast cancer cells after omega-3 PUFA incorporation, Cell Biochem. Biophys. 64 (2012) 45–59.
[27] I.A. Shaikh, I. Brown, K.W. Wahle, S.D. Heys, Enhancing cytotoxic therapies for breast and prostate cancers with polyunsaturated fatty acids, Nutr. Cancer 62 (2010) 284–296.
[28] S.C. Larsson, M. Kumlin, M. Ingelman-Sundberg, A. Wolk, Dietary long-chain n−3 fatty acids for the prevention of cancer: a review of potential mechanisms, Am. J. Clin. Nutr. 79 (2004) 935–945.
[29] P.A. Corsetto, G. Montorfano, S. Zava, I.E. Jovenitti, A. Cremona, B. Berra, A.M. Rizzo, Effects of n−3 PUFAs on breast cancer cells through their incorporation in plasma membrane, Lipids Health Dis. 10 (2011) 73.
[30] E. Cerf, R. Sarroukh, S. Tamamizu-Kato, L. Breydo, S. Derclaye, Y.F. Dufrêne, V. Narayanaswami, E. Goormaghtigh, J.M. Ruysschaert, V. Raussens, Antiparallel β-sheet: a signature structure of the oligomeric amyloid β-peptide, Biochem. J. 421 (2009) 415–423.
[31] H. Susi, D.M. Byler, Resolution-enhanced Fourier transform infrared spectroscopy of enzymes, Methods Enzymol. 130 (1986) 290–311.
[32] T.F. Cox, M.A.A. Cox, Multidimensional Scaling, Second edition Chapman and Hall/CRC, London, 2000.
[33] R Development Core Team, R: A Language and Environment for Statistical Computing, R Foundation for Statistical Computing, 2011.
[34] J.T.M. Pearce, Novel Computational Approaches to Characterising Metabolic Responses to Toxicity *via* an NMR-Based Metabonomic Database, University of London Imperial College London Biomolecular Medicine, 2010.
[35] J.O. Ramsay, Kernel smoothing approaches to nonparametric item characteristic curve estimation, Psychometrika 56 (1991) 611–630.
[36] G.P. Otto, B.J. Nichols, The roles of flotillin microdomains—endocytosis and beyond, J. Cell Sci. 124 (2011) 3933–3940.
[37] A. Natalello, D. Ami, S. Brocca, M. Lotti, S.M. Doglia, Secondary structure, conformational stability and glycosylation of a recombinant *Candida rugosa* lipase studied by Fourier-transform infrared spectroscopy, Biochem. J. 385 (2005) 511–517.
[38] K. Brandenburg, U. Seydel, Infrared spectroscopy of glycolipids, Chem. Phys. Lipids 96 (1998) 23–40.
[39] H.H. Mantsch, D.G. Cameron, P.A. Tremblay, M. Kates, Phosphatidylsulfocholine bilayers. An infrared spectroscopic characterization of the polymorphic phase behavior, Biochim. Biophys. Acta 689 (1982) 63–72.
[40] A. Natalello, F. Sasso, F. Secundo, Enzymatic transesterification monitored by an easy-to-use Fourier transform infrared spectroscopy method, Biotechnol. J. 8 (2013) 133–138.
[41] R.G. Sinclair, A.F. McKay, R.N. Jones, The infrared absorption spectra of saturated fatty acids and esters, J. Am. Chem. Soc. 74 (1952) 2570–2575.
[42] Z. Arsov, L. Quaroni, Detection of lipid phase coexistence and lipid interactions in sphingomyelin/cholesterol membranes by ATR-FTIR spectroscopy, Biochim. Biophys. Acta 1778 (2008) 880–889.
[43] J.A. Williams, S.E. Batten, M. Harris, B.D. Rockett, S.R. Shaikh, W. Stillwell, S.R. Wassall, Docosahexaenoic and eicosapentaenoic acids segregate differently between raft and nonraft domains, Biophys. J. 103 (2012) 228–237.
[44] F.S. Parker, Applications of Infrared Spectroscopy in Biochemistry, Biology, and Medicine, Plenum Press, New York, 1971.
[45] J.R. Silvius, Role of cholesterol in lipid raft formation: lessons from lipid model systems, Biochim. Biophys. Acta 1610 (2003) 174–183.